JACS
JOURNAL OF THE AMERICAN CHEMICAL SOCIETY

Communication

pubs.acs.org/JACS

An Optical Trap Combined with Three-Color FRET

Sanghwa Lee[†,‡] and Sungchul Hohng*[,†]

[†]Department of Physics and Astronomy, Department of Biophysics and Chemical Biology, and National Center for Creative Research Initiatives, Seoul National University, Seoul 151-747, Korea

Supporting Information

ABSTRACT: We developed a hybrid technique combining optical tweezers and single-molecule three-color fluorescence resonance energy transfer (FRET). In demonstrative experiments, we observed the force-sensitive correlated motion of three helical arms of a Holliday junction and identified the independent unfolding/folding dynamics of two DNA hairpins of the same length. With 3 times the number of observable elements of single-molecule FRET, this new instrument will enable the measurement of the complex, multidimensional effects of mechanical forces in various biomolecular systems, such as RNA and proteins.

Force plays crucial roles in many biomolecular processes. For the last two decades, single-molecule manipulation techniques, such as optical tweezers, magnetic tweezers, and atomic force microscopy, have enabled the observation of mechanical processes in real time with unprecedented accuracy and detail.[1] Using these techniques, scientists have characterized the mechanical properties of biomolecules, the effects of mechanical stress on biochemical reactions, and the operational mechanisms of molecular motors.[2−10] As a result, we have begun to understand the underlying mechanisms of several key biological processes.

Solely mechanical manipulation techniques, which usually probe only molecular end-to-end extension, have been fruitful for researchers. However, crucial details, such as the stoichiometries of active molecular complexes, and the internal conformations of molecular machines, are not directly accessible via these techniques. To circumvent these limitations and to detect molecular motions orthogonal to the direction of stretching, efforts have been made to combine mechanical manipulation tools with single-molecule fluorescence[11−13] and single-molecule fluorescence resonance energy transfer (FRET).[14−16] Using these hybrid techniques, important biological questions have been answered.[17−23]

Biological processes are frequently driven by molecular complexes with several components. Unfortunately, current hybrid techniques based on two-color FRET cannot capture the full complexity of many molecular systems. To overcome this limitation, we combined optical tweezers with single-molecule three-color FRET, allowing the determination of the force-dependent dynamics of three interdye distances. In demonstrative experiments, we observed the correlated motion of three helical arms of a Holliday junction under the application of force and the independent unfolding/folding dynamics of two DNA hairpins of the same length.

We built the hybrid instrument (Figure 1a) used in these experiments by modifying a commercial inverted microscope.

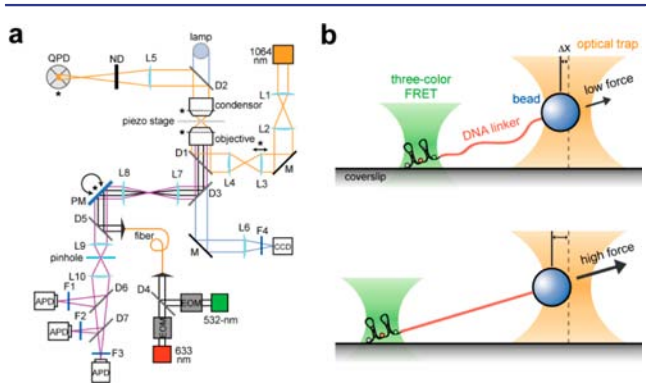

Figure 1. A hybrid instrument that combines optical tweezers with single-molecule three-color FRET. (a) Optical layout of the instrument. Detailed descriptions of the optical components are available in the Supporting Information. Light pathways are indicated for the 1064-nm trapping laser (orange), the 532-nm/633-nm fluorescence excitation lasers (black), fluorescence emission (purple), and halogen transillumination (light blue). For three-color FRET measurements, two excitation lasers were alternatively modulated by electrooptic modulators (EOMs). A quadrant photodiode (QPD) was used for bead position sensing, while three avalanche photodiodes (APDs) were used for single-molecule fluorescence detection. Conjugate image planes are indicated by asterisks. The incidence angle of the excitation beams (and thus, the excitation spot on the sample plane) is controlled by a piezo-controlled mirror (PM) to follow the motion of the immobilized molecules. Two telescopic lenses (L7 and L8) maintain the excitation beam intensity at varying incident angle. (b) Experimental scheme. A surface immobilized molecule with triplicate dye labeling is attached to a trapped bead via a long DNA linker. The long linker spatially separates the excitation beams (532 nm and 633 nm) from the trapping beam (1064 nm) to reduce dye photobleaching induced by the intensity of the trapping laser.

To trap a bead, an infrared laser was guided through the back port of the microscope and an objective lens. To monitor the position of the trapped bead, the infrared laser light scattered from the trapped bead was guided to a position detector via a condenser lens. The bead's position was measured by converting the voltage signals from the position detector, as previously described.[14,24] To facilitate the process of bead trapping, beads were visualized using an imaging system composed of a halogen lamp and a charge-coupled device

Received: August 23, 2013
Published: November 20, 2013

   dx.doi.org/10.1021/ja408767p | J. Am. Chem. Soc. 2013, 135, 18260−18263

camera. The single-molecule three-color FRET data were obtained using confocal microscopy. The setup is designed to detect Cy3, Cy5, and Cy7 fluorophores.[25] Green (532 nm) and red (633 nm) lasers were used to excite Cy3 and Cy5, respectively. To monitor the three interdye distances in real time, the two lasers were alternately switched on and off at a faster rate than the conformational dynamics of molecules.[25] To ensure that the two lasers illuminated the same molecules, the excitation lasers were coupled to a single mode fiber and guided through the same optical path to a sample. Cy3, Cy5, and Cy7 signals were collected by the objective lens and guided to avalanche photodiodes after being separated and filtered by dichroic mirrors and optical filters, respectively. From these fluorescence intensities, three FRET efficiencies were calculated, as previously described.[25]

In our experiments, a molecule labeled with FRET probes is immobilized on a polymer-coated glass surface and connected to an optical trap via a long DNA linker. To generate force, we move the surface to which the molecule is attached while maintaining the position of the trapping beam (Figure 1b). To obtain stable fluorescence signals regardless of molecular position, the fluorescence detection system follows molecular movements using a piezoelectric mirror mount (PM, Figure 1a). The angular position of the mirror mount is calibrated to the molecular position, as previously described.[14,24]

A Holliday junction is composed of four helical arms whose correlated motion has been well characterized by previous single-molecule FRET studies,[26,27] providing a good model system in which to test the capability of our hybrid instrument to measure simultaneously the force-dependence of multiple domain motions. We prepared a four-way DNA junction labeled with Cy3 (1st dye), Cy5 (2nd dye), and Cy7 (3rd dye) at each end of three helical arms (Figure 2a). The remaining arm was biotinylated for surface immobilization. The Cy7-labeled arm had a 12-nt single-stranded overhang, which was annealed to λ-phage DNA that was tethered to a trapped bead. A detailed description of the sample preparation process is available in the Supporting Information (SI). While the Holliday junction adopts two distinct stacking conformers (*isoI* and *isoII*) with similar probabilities in the absence of mechanical tension,[26,27] applied force is expected to bias the equilibrium toward *isoI* (Figure 2b).

Figure 2c shows examples of single-molecule fluorescence intensity time traces at 0.7 pN for Cy3 excitation (top panel) and Cy5 excitation (bottom panel). Three interdye FRET efficiencies (E_{12}: FRET efficiency for the Cy3-Cy5 pair, E_{23}: FRET efficiency for the Cy5-Cy7 pair, E_{13}: FRET efficiency for the Cy3-Cy7 pair) calculated from the data in Figure 2c are shown in Figure 2d.[25] E_{12} and E_{23} exhibited clear two-state dynamics between *isoI* (E_{12}: low, and E_{23}: high) and *isoII* (E_{12}: high, E_{23}: low), while E_{13} remained approximately equivalent between the two conformations. As expected, the relative distribution of E_{12} and E_{23} at different forces exhibited a force-induced bias toward the *isoI* state (Figure 2e). The probability of obtaining the *isoI* state as a function of force (F) was fit to a Boltzmann function $p_I(F) = \{1 + \exp((F_{1/2} - F)\cdot\Delta x/(k_BT))\}^{-1}$ (Figure 2f), where $F_{1/2}$ is the force at which the Holliday junction has a 50% probability of being in the *isoI* state.[28,29] We found $F_{1/2}$ = 0.06 pN and Δx = 5.9 nm, which are in good agreement with the values previously reported.[14]

As a second demonstration, we studied the force-induced unfolding/folding dynamics of two independent DNA hairpins. We prepared a DNA construct containing two DNA hairpins

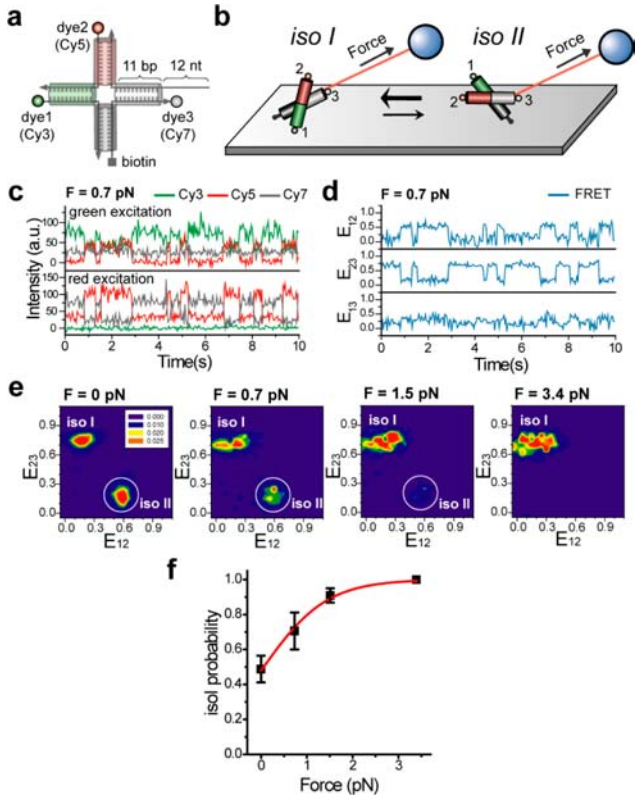

Figure 2. Conformational dynamics of a triple-labeled Holliday junction as a function of the applied force. (a) Labeling scheme of the Holliday junction. (b) Illustration of the experimental design. When force is applied to the Holliday junction as shown in the scheme, the *isoI* form is more prevalent than the *isoII* form. (c) Representative fluorescence intensity time traces of the Holliday junction for green (top) and red (bottom) excitations at 0.7 pN. Fluorescence signals of Cy3, Cy5, and Cy7 are green, red, and gray, respectively. (d) Three FRET efficiency time traces calculated from the data in (c). (e) Relative distribution of E_{12} and E_{23} at varying forces. Consistent with our expectations, the distribution is biased toward *isoI* at high forces. Histograms were constructed from two repeated measurements of the same molecule. (f) The probability of *isoI* (black) as a function of force and a fit of the data to a two-state Boltzmann function (red). Experiments were performed at room temperature in 10 mM Tris-HCl (pH 8.0) with 50 mM Mg^{2+}. The error bars were made from repeated measurements of two molecules.

(H1 and H2) (Figure 3a). To observe the unfolding/folding dynamics of the two hairpins via FRET, the DNA construct was labeled with Cy3, Cy5, and Cy7 such that E_{12} and E_{23} report the folding/unfolding of H1 and H2, respectively. Because the two hairpins have the same length (an 8-bp stem and a 10-nt thymine loop) and similar stabilities, it is not possible to tell which hairpin is unfolded by force solely via mechanical manipulation techniques. To apply force, the immobilized DNA construct was attached to a trapped bead via a λ-phage DNA (Figure 3b). A detailed description of the sample preparation process is available in the SI.

Figure 3c shows representative fluorescence intensity time traces at 9.8 pN for Cy3 excitation (top panel) and Cy5 excitation (bottom panel). E_{12} and E_{23} calculated from the data in Figure 3c are shown in Figure 3d. Although the unfolding and folding of H1 and H2 are independent and stochastic, we could clearly distinguish the folding/unfolding states of H1 and H2. Figure 3e shows the equilibrium constants of the unfolded

dx.doi.org/10.1021/ja408767p | J. Am. Chem. Soc. 2013, 135, 18260−18263

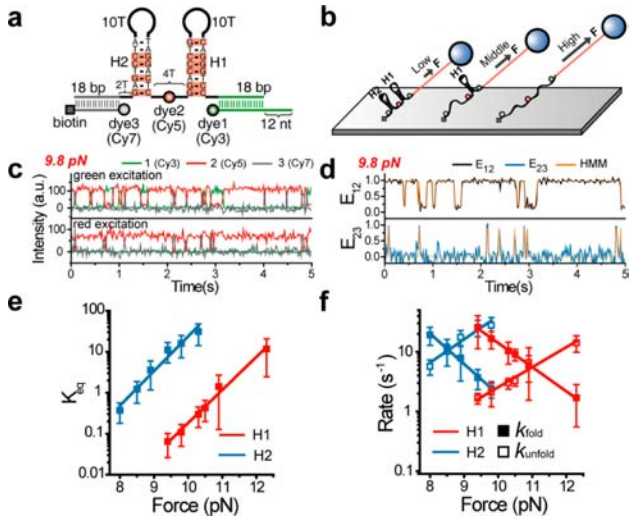

Figure 3. Force-induced unfolding/folding dynamics of DNA hairpins. (a) DNA construct used for the experiments. The two DNA hairpins have the same length and slightly different GC contents. The Cy3-Cy5 FRET pair is designed to monitor the unfolding of H1 while the Cy5-Cy7 FRET pair monitors the unfolding of H2. (b) Experimental scheme. H2 has a lower GC content than H1, and is expected to unfold at lower forces. (c) Representative fluorescence intensity time traces for green (top) and red excitations (bottom) at 9.8 pN. Fluorescence signals of Cy3, Cy5, and Cy7 are colored green, red, and gray, respectively. (d) FRET efficiency time traces (E_{12}: top, E_{23}: bottom) obtained from the data in (c). Orange lines are the most probable FRET trajectories generated by hidden Markov modeling.[32] (e) The equilibrium constant of the unfolded state (K_{eq}: the ratio of the unfolded state population to the folded state population) as a function of force for H1 (red) and H2 (blue). The error bars were made from repeated experiments of 10 molecules (SI, Figure S1). (f) Rate constants of folding/unfolding reactions as functions of force. Transition rates for the folding and unfolding of both hairpins are determined from hidden Markov modeling. The error bars were made from repeated experiments of 10 molecules (SI, Figure S2). To obtain distances to the transition state, data were fit to a linear equation on a log−linear scale.

states as a function of force for H1 and H2. Consistent with the fact that H1 has a higher GC content (75%) than H2 (50%), the unfolding force ($F_{1/2}$: the force at which a DNA hairpin has a 50% probability of being unfolded) of H1 is higher than that of H2 (10.9 pN and 8.4 pN, respectively). Figure 3f shows the folding/unfolding transition rate as a function of force. The data were fit to $k = k_0 \exp(-F\Delta x^{\ddagger}/k_B T)$, where $\Delta x^{\ddagger}$ is the distance to the transition state and k_0 is the transition rate at a force of zero.[28,29] The parameters determined from Figure 3e,f (Table 1) are consistent with previously reported values.[30] We also performed similar experiments with a different DNA construct that has fast unfolding/folding dynamics of DNA hairpins. Though kinetic information of unfolding/folding reactions were not accessible, the unfolding forces of two different hairpins could be independently determined via FRET histogram shift (Figure S3 in SI).

In summary, we successfully combined optical tweezers and single-molecule three-color FRET. While current hybrid techniques monitor only a single interdye distance, this new instrument triples the number of observable elements, which allows the monitoring of the complex, multidimensional effects of mechanical force on DNA molecules. With minor modifications, our method can be readily applied to other nucleic acid systems. With the advent of orthogonal labeling techniques,[31] this hybrid instrument can be used to study multistep protein folding/unfolding processes as well as the dynamic interactions of protein complexes under force.

Table 1. Kinetic Parameters of the Hairpins Measured from the Force-Dependent Transition Rates for the Folding and Unfolding Reactions

hairpins	$\Delta x^{\ddagger}_{u\to f}$ (nm)	$\Delta x^{\ddagger}_{f\to u}$ (nm)	Δx_{eq} (nm)	$F_{1/2}$ (pN)
H1	3.83	3.17	7.0 (7.62)[a]	11.0 (10.9)[a]
H2	4.82	3.71	8.53 (8.01)[a]	8.5 (8.4)[a]

hairpins	folding rate at $F = 0$ (s^{-1})	unfolding rate at $F = 0$ (s^{-1})	folding lifetime at $F_{1/2}$ (s)
H1	1.58×10^5	1.13×10^{-3}	0.18
H2	2.43×10^5	4.87×10^{-3}	0.09

[a]These values were obtained from Figure 3e. All other values were obtained from Figure 3f.

■ ASSOCIATED CONTENT

Ⓢ Supporting Information

Materials and detailed experimental methods, and supplementary figures. This material is available free of charge via the Internet at http://pubs.acs.org.

■ AUTHOR INFORMATION

Corresponding Author

shohng@snu.ac.kr

Present Address

‡Biomedical Research Institute, Korea Institute of Science and Technology, Seoul 136-791, South Korea.

Notes

The authors declare no competing financial interest.

■ ACKNOWLEDGMENTS

We thank all of the members of our lab for their kind discussion and help. This work was supported by Creative Research Initiatives (2009-0081562) of the National Research Foundation of Korea.

■ REFERENCES

(1) Neuman, K. C.; Nagy, A. *Nat. Methods* **2008**, *5*, 491.
(2) Fernandez, J. M.; Li, H. *Science* **2004**, *303*, 1674.
(3) Greenleaf, W. J.; Woodside, M. T.; Block, S. M. *Annu. Rev. Biophys. Biomol. Struct.* **2007**, *36*, 171.
(4) Herbert, K. M.; Greenleaf, W. J.; Block, S. M. *Annu. Rev. Biochem.* **2008**, *77*, 149.
(5) Moffitt, J. R.; Chemla, Y. R.; Smith, S. B.; Bustamante, C. *Annu. Rev. Biochem.* **2008**, *77*, 205.
(6) Meglio, A.; Praly, E.; Ding, F.; Allemand, J. F.; Bensimon, D.; Croquette, V. *Curr. Opin. Struct. Biol.* **2009**, *19*, 615.
(7) Bustamante, C.; Cheng, W.; Mejia, Y. X. *Cell* **2011**, *144*, 480.
(8) Killian, J. L.; Li, M.; Sheinin, M. Y.; Wang, M. D. *Curr. Opin. Struct. Biol.* **2012**, *22*, 80.
(9) De Vlaminck, I.; Dekker, C. *Annu. Rev. Biophys.* **2012**, *41*, 453.
(10) Dulin, D.; Lipfert, J.; Moolman, M. C.; Dekker, N. H. *Nat. Rev. Genet.* **2013**, *14*, 9.
(11) Ishijima, A.; Kojima, H.; Funatsu, T.; Tokunaga, M.; Higuchi, H.; Tanaka, H.; Yanagida, T. *Cell* **1998**, *92*, 161.
(12) Lang, M. J.; Fordyce, P. M.; Engh, A. M.; Neuman, K. C.; Block, S. M. *Nat. Methods* **2004**, *1*, 133.
(13) Comstock, M. J.; Ha, T.; Chemla, Y. R. *Nat. Methods* **2011**, *8*, 335.

(14) Hohng, S.; Zhou, R.; Nahas, M. K.; Yu, J.; Schulten, K.; Lilley, D. M.; Ha, T. *Science* **2007**, *318*, 279.
(15) Tarsa, P. B.; Brau, R. R.; Barch, M.; Ferrer, J. M.; Freyzon, Y.; Matsudaira, P.; Lang, M. J. *Angew. Chem., Int. Ed.* **2007**, *46*, 1999.
(16) Shroff, H.; Reinhard, B. M.; Siu, M.; Agarwal, H.; Spakowitz, A.; Liphardt, J. *Nano Lett.* **2005**, *5*, 1509.
(17) van Mameren, J.; Modesti, M.; Kanaar, R.; Wyman, C.; Peterman, E. J.; Wuite, G. J. *Nature* **2009**, *457*, 745.
(18) van Mameren, J.; Gross, P.; Farge, G.; Hooijman, P.; Modesti, M.; Falkenberg, M.; Wuite, G. J.; Peterman, E. J. *Proc. Natl. Acad. Sci. U. S. A.* **2009**, *106*, 18231.
(19) Lee, M.; Kim, S. H.; Hong, S. C. *Proc. Natl. Acad. Sci. U. S. A.* **2010**, *107*, 4985.
(20) Zhou, R.; Kozlov, A. G.; Roy, R.; Zhang, J.; Korolev, S.; Lohman, T. M.; Ha, T. *Cell* **2011**, *146*, 222.
(21) Long, X.; Parks, J. W.; Bagshaw, C. R.; Stone, M. D. *Nucleic Acids Res.* **2013**, *41*, 2746.
(22) Schwarz, F. W.; Toth, J.; van Aelst, K.; Cui, G.; Clausing, S.; Szczelkun, M. D.; Seidel, R. *Science* **2013**, *340*, 353.
(23) Lee, K. S.; Balci, H.; Jia, H.; Lohman, T. M.; Ha, T. *Nat. Commun.* **2013**, *4*, 1878.
(24) Zhou, R.; Schlierf, M.; Ha, T. *Methods Enzymol.* **2010**, *475*, 405.
(25) Lee, S.; Lee, J.; Hohng, S. *PLoS One* **2010**, *5*, e12270.
(26) McKinney, S. A.; Declais, A. C.; Lilley, D. M.; Ha, T. *Nat. Struct. Biol.* **2003**, *10*, 93.
(27) Joo, C.; McKinney, S. A.; Lilley, D. M.; Ha, T. *J. Mol. Biol.* **2004**, *341*, 739.
(28) Liphardt, J.; Onoa, B.; Smith, S. B.; Tinoco, I., Jr.; Bustamante, C. *Science* **2001**, *292*, 733.
(29) Bustamante, C.; Chemla, Y. R.; Forde, N. R.; Izhaky, D. *Annu. Rev. Biochem.* **2004**, *73*, 705.
(30) Woodside, M. T.; Behnke-Parks, W. M.; Larizadeh, K.; Travers, K.; Herschlag, D.; Block, S. M. *Proc. Natl. Acad. Sci. U.S.A.* **2006**, *103*, 6190.
(31) Kim, J.; Seo, M. H.; Lee, S.; Cho, K.; Yang, A.; Woo, K.; Kim, H. S.; Park, H. S. *Anal. Chem.* **2013**, *85*, 1468.
(32) McKinney, S. A.; Joo, C.; Ha, T. *Biophys. J.* **2006**, *91*, 1941.